

**LIQUID PHASE ISOPHORONE OXIDE REARRANGEMENT OVER MESOPOROUS
Al-MCM-41 MATERIALS**

Rafael van Grieken, David P. Serrano, Juan Antonio Melero* and Alicia García
Chemical and Environmental Engineering Group, ESCET, Rey Juan Carlos University,
C/ Tulipán s/n, 28933, Móstoles, Spain.

Published on:

Journal of catalysis, 236 (2005) 122-128

[doi:10.1016/j.jcat.2005.09.028](https://doi.org/10.1016/j.jcat.2005.09.028)

*Corresponding author

Tel: +34 91 488 70 87. Fax: +34 91 488 70 68

e-mail address: juan.melero@urjc.es

Abstract

The rearrangement of isophorone oxide has been investigated over Al-MCM-41 type mesostructured catalysts having different Si/Al molar ratios. The main rearrangement products are the α -diketone and the keto aldehyde, whereas the product coming from the decarbonylation of the latter is detected in minor amounts. The textural properties and the number of acid sites of Al-MCM-41 materials influence the extent of isophorone oxide rearrangement reaction. The best catalytic performance in regards to epoxide conversion is obtained for a catalyst having a molar Si/Al ratio around 40 due to a right contribution of acid site concentration and pore size. However, irrespective to the aluminium content of the catalysts and the reaction temperature, the selectivity to the desired keto aldehyde was around 80%. Al-MCM-41 materials are superior catalysts compared to zeolites in terms of both activity and aldehyde selectivity. As a consequence of its large pore size, the use of Al-containing mesostructured materials as catalyst in isophorone oxide rearrangement allows the diffusional problems present in zeolites to be avoided.

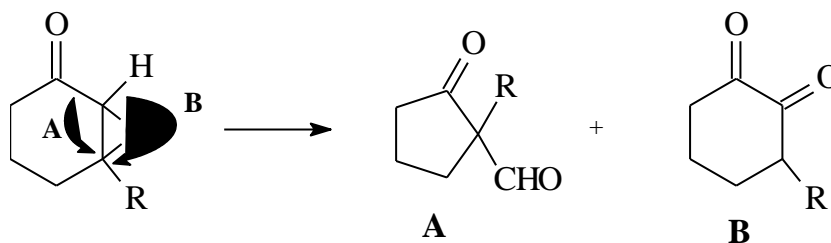
Keywords: isophorone oxide, rearrangement, epoxide, mesostructured materials, Al-MCM-41

1. Introduction

The catalytic rearrangement of epoxides, leading to useful intermediates in organic syntheses, has been widely studied over both homogeneous and heterogeneous catalysts [1, 2]. Acidic activation of epoxides for ring opening reactions leading to aldehydes, ketones, ethers or alcohols can be achieved either by Brønsted acid catalysts via addition of a proton to the epoxide oxygen or by Lewis acid catalysts via coordination of the epoxide oxygen to a multivalent cation [3]. The use of zeolitic materials as catalysts for the epoxide rearrangement reactions presents as main advantage their well defined pore system compared with homogeneous systems or other heterogeneous catalysts such as metal oxides (e.g. silica and alumina), metal sulfates or precipitated phosphates [4]. Indeed, zeolites in their proton form (e.g. ZSM-5) as well as the weakly Lewis-acidic titanium containing zeolites (e.g. TS-1 and Ti-Beta) have been found to catalyze this type of reactions [5].

Cyclic α,β -epoxy ketones are interesting intermediates in organic synthesis since they are very reactive compounds. Several products resulting from the rearrangement of such epoxides are valuable raw materials for the preparation of perfumes, synthetic food flavourings and pharmaceuticals [6, 7]. The rearrangement of α,β -epoxy ketones was originally investigated by House *et al.* using homogeneous Lewis acids as catalysts [8]. The cyclic α,β -epoxy ketones are rearranged via an intramolecular reaction to aldehydes and diones using boron trifluoride etherate as homogeneous catalyst. In the presence of Lewis acids the oxirane ring is cleaved at the β -carbon atom as depicted in Scheme 1. Cleavage at the α -carbon is energetically unfavourable since it generates partial positive charges on adjacent atoms [9]. Cleavage is followed by acyl or hydrogen migration (route A and B, respectively). Acyl migration results in ring contraction to yield the aldehyde, a reaction pathway favoured over hydrogen migration

when $\text{BF}_3 \cdot \text{Et}_2\text{O}$ is used as catalyst, particularly if an additional substituent is present at the β -position [10].



Scheme 1. Lewis acid catalysed rearrangement of a cyclic α,β -epoxy ketone. (A) Acyl migration (B) hydrogen migration.

Heterogeneous catalysts have scarcely been used in the rearrangement of α,β -epoxy ketones, in spite of their advantages regarding the ease of recovery and recycling. Rao and Rao studied the rearrangement of highly active chalcone oxides to 1,3-diphenylpropane-1,2-diones at room temperature using silica gel as catalyst [11]. Meyer *et al.* reported liquid and vapour phase rearrangement of isophorone oxide with high yields (up to 80%) to keto aldehyde over zeolitic materials [12]. Recently, Elings *et al.* [13] have investigated the rearrangement of various cyclic α,β -epoxy ketones (isophorone oxide, 2,3-epoxy-3-methylcyclohexan-1-one or pulegone oxide) with the use of solid acids catalysts, including silica, zeolites and clays as an alternative to the classical homogeneous $\text{BF}_3 \cdot \text{Et}_2\text{O}$ system.

Zeolites are microporous materials having limited pore size that lead to strong diffusional hindrances for both reactants and products and fast deactivation. Therefore, in presence of bulky compounds the activity of zeolites is restricted to the active sites located on the external surface. In this context compared to zeolites, the mesoporous MCM-41 materials discovered by the researchers of Mobil Oil Company [14] may be convenient catalysts in processes involving high volume molecules as they possess high surface area and large mesopore diameters. Indeed, the presence of Al atoms incorporated into the walls turned these materials into solids with acid sites of medium strength with potential applications for the

catalytic conversion of bulky molecules [15, 16]. Moreover, these catalysts can be synthesized over a wide range of Si/Al ratios, which makes possible to modify and adjust their acidic properties.

Recently, Al-containing MCM-41 materials were reported to be more effective catalysts for both liquid and vapour-phase Beckmann rearrangement of cyclohexanone oxime in comparison to zeolites and other mesoporous catalysts [17, 18]. Although, works dealing with the use of solid acids in Claisen rearrangement are rather scarce, Mathew *et al.* have reported the use of Al-MCM-41 with different Si/Al ratios in the rearrangement of allyl phenyl ether and they observed a close relationship between acidity and conversion [19]. Moreover, α -pinene oxide rearrangement to campholenic aldehyde in liquid phase over Al-MCM-41 type mesostructured materials has already been documented in the literature [20]. In this work a high conversion was observed in comparison to other catalysts such as SiO₂, B₂O₃/SiO₂ or ZnCl₂, but the selectivity was dependent on the aluminium content, varying from 49 to 66%.

We have recently studied the catalytic rearrangement of 1,2-epoxyoctane in liquid phase over different solid catalysts, having a variety of acid properties and structural features, including diverse zeolites and mesostructured materials [21-22]. The mesoporous materials present much higher activities per active site in comparison to those obtained with zeolitic materials, probably arising from its larger pore sizes. These previous works prompted us to apply Al-MCM-41 type mesostructured materials as catalysts in the rearrangement of epoxides of different nature, with application in Fine Chemistry. In the present manuscript we report for the first time the catalytic performance of Al-MCM-41 materials with different Si/Al molar ratios on the liquid-phase isophorone oxide rearrangement.

2. Experimental

2.1. Synthesis and characterization of catalysts

Al-containing MCM-41 type catalysts with Si/Al ratios ranging from 5 to 100 were prepared in our laboratory according to a sol-gel procedure at room temperature published elsewhere [23]. Two solutions were prepared under gentle stirring: solution A, formed by 20 g of tetraethylorthosilicate (TEOS; Alfa) and aluminium isopropoxide (AIP; Aldrich; from 0.2 to 3.9 g depending on the initial Si/Al molar ratio in the synthesis gel), and solution B, formed by 36.5 g of hexadecyltrimethylammonium chloride (CTACl; Aldrich) and 6.6 g of hydrogen chloride. Once these solutions were perfectly homogenised, solution A was added to solution B and the mixture was kept under stirring at room temperature for 75 min. Thereafter, 54 g of a 2 wt.% aqueous ammonia solution were added dropwise and stirred for 1 h. The obtained sample was filtered, washed with deionized water and dried at 110°C for 12 h. The final product was obtained by calcination in static air at 550°C for 12 h.

The catalytic samples synthesized were characterized by different techniques. Mesoscopic ordering was checked through X-Ray diffraction (XRD) patterns acquired with a Philips X'PERT MPD diffractometer using Cu K α radiation. Typically, the data were collected from 0.6° to 10° (2 θ) with a resolution of 0.02°. The Si/Al atomic ratio of the calcined samples was obtained by induced coupled plasma-atomic emission spectroscopy (ICP-AES) with a Varian VISTA-AX apparatus. Textural properties of catalysts were determined by means of nitrogen adsorption-desorption isotherms at 77 K with a Micromeritics ASAP 2010 porosimeter after outgassing of the calcined samples under vacuum at 200 °C for 5 h. The surface areas were obtained according to the BET equation whereas the pore size distribution in the mesopore

region was determined applying the BJH method to the adsorption branch of the isotherm. The total pore volume was calculated from the nitrogen adsorption at $p/p_0=0.99$.

The coordination of aluminium atoms in the framework of the solids was checked by ^{27}Al -MAS-NMR spectra of the calcined samples. The spectra were recorded at 104.26 MHz in a VARIAN Infinity 400 spectrometer at spinning frequency of 4 KHz. Intervals of 30 s between successive accumulations were selected. The external standard reference was $[\text{Al}(\text{H}_2\text{O})_6^{+3}]$ and all measurements were carried out at room temperature. Catalyst acidity was determined by ammonia temperature programmed desorption (TPD) in a Micromeritics 2910 (TPD/TPR) equipment. Previously, the samples were outgassed under a helium flow (50 Nml min^{-1}) with a heating rate of $15 \text{ }^\circ\text{C min}^{-1}$ up to $560 \text{ }^\circ\text{C}$ and kept at this temperature for 30 min. After cooling to $180 \text{ }^\circ\text{C}$, an ammonia flow of 35 Nml min^{-1} was passed through the sample for 30 min. The physisorbed ammonia was removed by flowing helium at $180 \text{ }^\circ\text{C}$ for 90 min. The desorption of the chemically adsorbed ammonia was monitored while increasing the temperature up to $560 \text{ }^\circ\text{C}$ with a heating rate of $15 \text{ }^\circ\text{C min}^{-1}$, this temperature being kept for 30 min. The ammonia concentration in the effluent stream was measured by means of a thermal conductivity detector (TCD).

2.2. Catalytic Experiments

The catalytic experiments were carried out at 80°C in a 0.1 L stirred batch autoclave, equipped with a temperature controller and a pressure gauge under stirring (550 rpm) and autogenous pressure. This experimental set-up is also provided with a device to feed the epoxide into the teflon-lined reactor once the reaction temperature is reached. The solvent and the catalyst are initially placed in the teflon-lined reactor. The zero time of the reaction is taken when the temperature reaches the set-point value and the epoxide is loaded into the reactor. The composition of the reaction mixture was as follows: 1.25 g of isophorone oxide, 50 g of toluene

(water content less than 0.03 wt.%) and 0.1 g of catalyst. Toluene was stored with zeolite A to minimise its water content. The catalyst, prior reaction, was dried overnight at 140°C to remove adsorbed water.

The reaction products were analyzed with a VARIAN 3800 chromatograph equipped with a capillary column (HP-FFAP) with dimensions 60 x 0.32 mm, using a flame ionization detector (FID). Identification of the different reaction products was performed by mass spectrometry (VARIAN SATURN 2000) using standard compounds.

3. Results and discussion

3.1 Catalysts properties

The main physicochemical and textural properties of the Al-MCM-41 materials prepared in this work are summarized in Table 1. Chemical analysis of calcined samples gives molar Si/Al ratios higher than those present in the starting synthesis mixture, although aluminium incorporation degree is enhanced at low Al content. Starting from a Si/Al molar ratio of 100 the incorporation is ca. 90 % whereas from initial Si/Al molar ratios of 5 and 20 the incorporation degree decreases up to ca. 37 and 50 % respectively. However, a question to be considered is whether this aluminium is tetrahedrally incorporated into the silica framework. As-synthesised materials exhibit a unique signal centred at 50 ppm in the ^{27}Al MAS-NMR spectra indicating a tetrahedral environment of Al atoms regardless of their content in the synthesis medium. In contrast, ^{27}Al MAS-NMR spectra of the samples after calcination in air at 550°C exhibit two clear peaks centred at ~0 and ~50 ppm originated from octahedrally and tetrahedrally coordinated aluminium species, respectively (Figure 1). The relative proportion of octahedral aluminium increases as the molar Si/Al ratio of the catalyst decreases, although its

contribution is always clearly lower than the one corresponding to tetrahedral aluminium for the three samples. These results show that the incorporation of aluminium atoms in MCM-41 silica walls is hindered as the aluminium content in the synthesis mixture increases.

Table 1. Physicochemical properties of the Al-MCM-41 type catalysts.

Catalysts	Al-MCM-41 (1)	Al-MCM-41 (2)	Al-MCM-41 (3)
Si/Al (starting composition)	5	20	100
Si/Al (calcined sample)	14	38	114
D_{BJH} (nm) ^a	< 2.0	2.3	2.5
D_p (nm) ^b	1.9	3.0	3.1
Surface Area (m ² g ⁻¹)	720	1049	1115
Pore Volume (cm ³ g ⁻¹) ^c	0.34	0.78	0.87
Acidity (mmol g ⁻¹) ^d	0.52	0.23	0.11
T maximum (°C) ^d	266	268	270
Al (mmol Al g ⁻¹) ^e	1.15	0.43	0.15

^a Maximum in pore size distribution calculated from the adsorption branch with BJH method

^b Pore diameter calculated assuming cylindrical geometry as D_p (nm) = 4 * Pore volume (cm³/g) / Surface area (m²/g)*1000

^c Total pore volume measured at P/P₀ = 0.99.

^d Calculated from ammonia TPD measurements.

^e Total aluminium species per g of calcined sample.

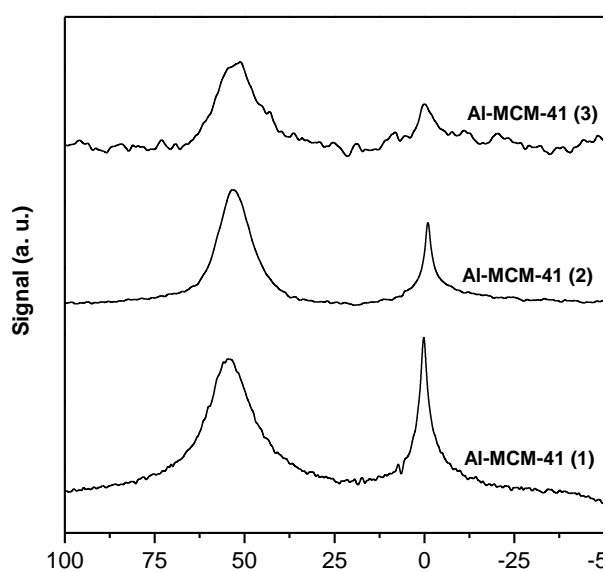


Figure 1. ²⁷Al MAS-NMR spectra of calcined samples.

For all the calcined samples, the XRD spectra (Figure 2) show solely a main peak in the range 2.7-3.5 nm ($2\theta = 3.29\text{-}2.49^\circ$) corresponding to the d_{100} reflection of 2D hexagonal symmetry, whose intensity varies slightly with the aluminium content. In general, the d-spacing at $2\theta \cong 3$ decreases with increasing aluminium content ($d = 3.5, 3.3$ and 2.7 nm for Si/Al = 100, 20 and 5, respectively) and less resolved XRD patterns are obtained. Additional peaks are not observed indicating the absence of long range order. Therefore, larger amounts of aluminium incorporated in the pore walls cause a decrease in the long range order in Al-containing MCM-41 materials [23].

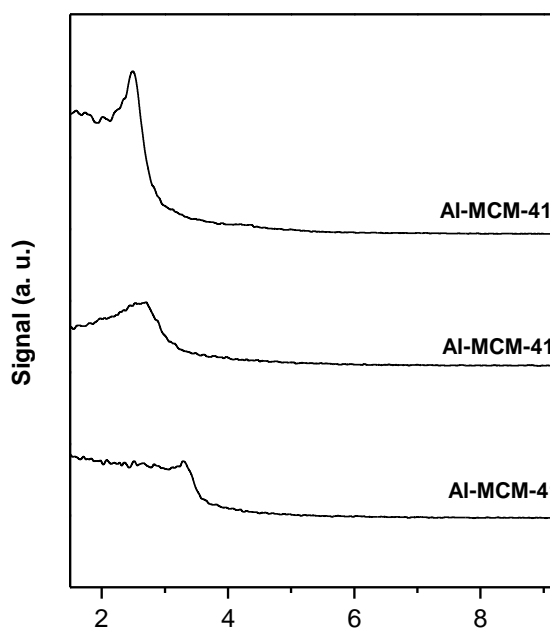


Figure 2. XRD spectra of calcined samples.

Figure 3 exhibits the nitrogen adsorption isotherms at 77 K for the three calcined samples Al-MCM-41 (1), (2) and (3) and their respective pore size distributions. The samples Al-MCM-41 (2) and (3) present a type IV isotherm in the IUPAC classification, typical for mesoporous materials. As common features in the isotherms of both samples, it is noteworthy a mono-multilayer adsorption zone at low relative pressures, a distinct jump of capillary condensation in mesopores at $P/P_0 = 0.1\text{-}0.4$ and an almost constant adsorption zone at high

relative pressures due to multilayer adsorption on the particle surface. The inflection point of these isotherms is situated at $P/P_0 \sim 0.25$, and the different stages are clearly separated. This is not the case with the adsorption isotherm for the Al-MCM-41 (1) sample as it does not show capillary condensation in the mesopores, just mono-multilayer adsorption or micropore filling being observed. This isotherm could be classified as type I following IUPAC criteria and it is typical for microporous materials. These types of isotherms have been previously reported for MCM-41 materials with small pore sizes, synthesized through a sol-gel route based on the use of short chain cationic surfactants [24]. The decrease of the pore size at high Al contents is in agreement with the reduction in the d-spacing observed in the XRD spectra.

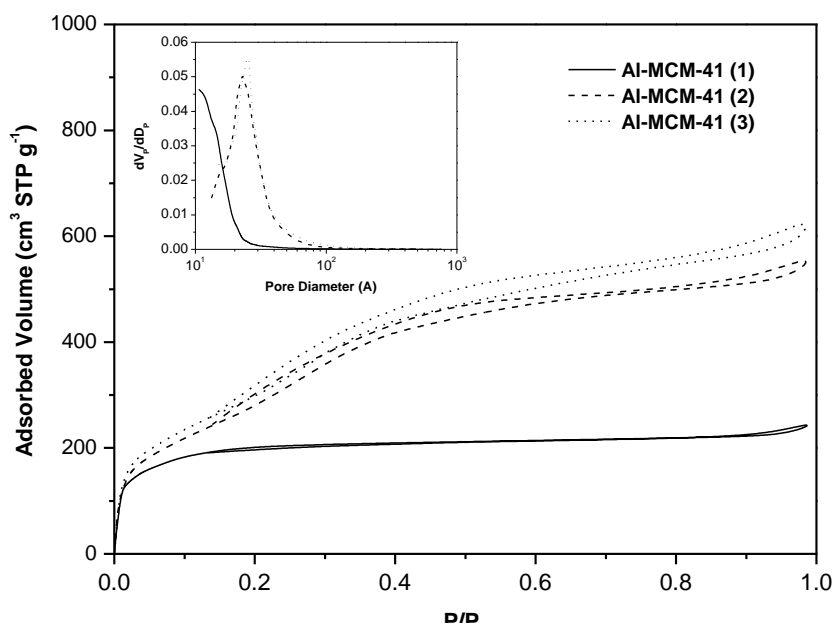


Figure 3. Nitrogen adsorption isotherms at 77 K and BJH pore size distributions (left top) of calcined samples.

BET surface area, pore volume and the average pore size present a common trend, with a continuous rise as the molar Si/Al ratio is increased (see Table 1). Thus, the BET surface area values increase from 720 to 1115 $\text{m}^2 \text{g}^{-1}$, the pore volume (measured at $P/P_0 = 0.99$) from 0.34 to 0.87 $\text{cm}^3 \text{g}^{-1}$ and the average pore size from less than 2.0 nm to 2.5 nm. Therefore, the

aluminium content has a strong influence on the textural properties of the material finally obtained, since it leads to a change from mesoporous materials, Al-MCM-41 (3) and (2), to a microporous one ($D_p < 2.0$ nm) in the case of the Al-MCM-41 (1) sample.

The acid properties of Al-MCM-41 samples have been investigated by means of NH_3 TPD analysis (Figure 4), the results being reported in Table 1. As expected, the number of acid sites increases with the aluminium content incorporated within the mesoscopic structure (see data in Table 1). Nevertheless, data in Table 1 indicates that there are a number of Al atoms not accessible to ammonia molecules. This accessibility is clearly enhanced as the Al content is lower in the synthesis mixture reaching the highest values for the material synthesized with an initial molar ratio of 100. Chemical and NH_3 TPD analysis clearly indicate that low Al contents in the synthesis mixture favours incorporation and accessibility of Al atoms in the mesoscopic structure. All samples, show the presence of sites with medium acid strength as indicated by the temperature maximum of ammonia desorption within the range 266-270°C. Regardless of their aluminium content, all the samples present acid sites of similar strength at least based on the data obtained from TPD measurements. Additionally, all the samples also show one-two shoulders in the main signal at temperatures over 450 °C probably arising from dehydroxilation processes promoted at high temperatures.

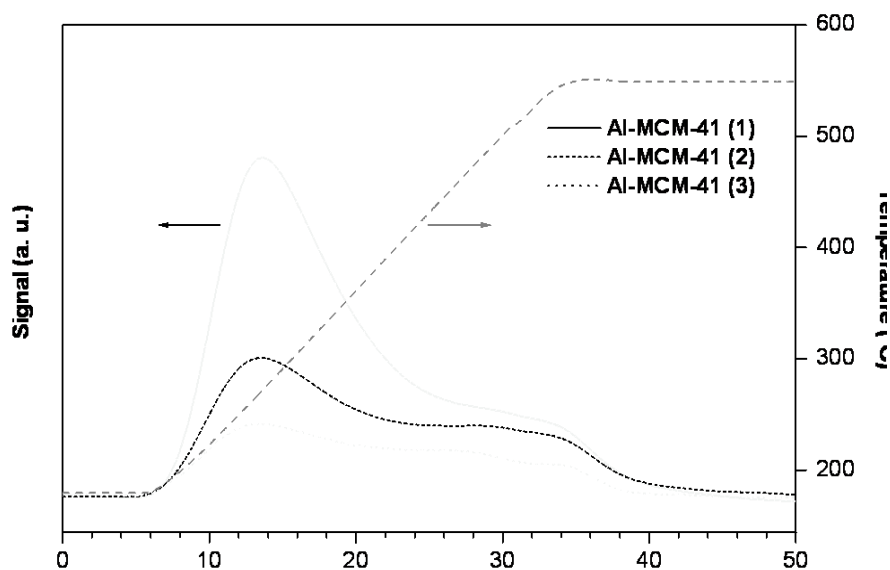
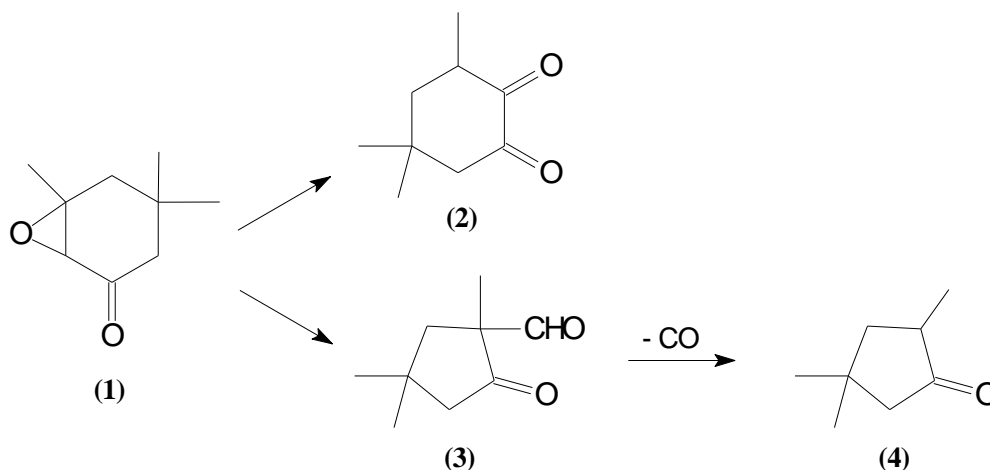


Figure 4. NH₃ TPD of calcined samples.

3.2. Catalytic epoxide rearrangement

Rearrangement of isophorone oxide (1) yields, as major products, the α -diketone (2) and the keto aldehyde (3), whereas the formation of (4) can be explained by deformylation of (3) as depicted in Scheme 2 [5]. From an industrial point of view the desired compound is the keto aldehyde, which is an interesting intermediate for the synthesis of other cyclopentanone derivatives with floral and fruity smells. The acid catalyzed reaction mechanism leading to the synthesis of keto aldehyde (2) had been earlier discussed for homogeneous catalysts [25]. Therefore, it is of interest whether the product distribution changes in the presence of a heterogeneous catalyst system and also whether the decarbonylation of the compound (3) to compound (4) can be suppressed.



Scheme 2. Rearrangement of isophorone oxide (1) to 3,5,5-trimethyl-1,2-cyclohexanedione (2) and 2-formyl-2,4,4-trimethylcyclopentanone (3) and subsequent deformylation of (3) to 2,4,4-trimethylcyclopentanone (4).

The epoxide conversion results obtained over the different Al-MCM-41 samples in the rearrangement of isophorone epoxide in liquid phase are shown in Figure 5. Since some epoxides may be isomerised thermally, a blank reaction in absence of catalyst was carried out that yielded a negligible conversion under the reaction conditions used in this work. However, when Al-MCM-41 materials are used as catalysts, the epoxide conversion increases significantly with the reaction time. The highest values were obtained over Al-MCM-41 (2) material (molar Si/Al ratio: 38), for which the epoxide conversion reached around 60% for the first 25 minutes of reaction, increasing up to 90% in 2 hours.

The low conversion observed with Al-MCM-41 (1) (molar Si/Al ratio: 14; $D_p < 2.0$ nm) in comparison to that obtained with Al-MCM-41 (2) ($D_p > 2.0$ nm), is presumably due to its lower average pore size which hinders the accessibility of the epoxide to the active sites of the catalyst and the diffusion of products out of the pore system. It is worthy to remark the epoxide conversion values obtained over Al-MCM-41 (3) catalyst (molar Si/Al ratio: 114; $D_p > 2.0$ nm), since greater values should be expected considering the large pore diameter of this material. This fact might be attributed to the lower aluminium content of this catalyst that leads to a decrease of the number of active sites present on its surface. Therefore, the extent of isophorone

oxide rearrangement reaction seems to be clearly influenced by textural properties, as well as by the number of acid sites present in Al-MCM-41 materials used as catalysts. In this sense, a Si/Al molar ratio of ca. 40 can be considered optimal aluminium content of the Al-MCM-41 catalyst which allows a right combination of pore size and acid site concentration to be attained.

For all the samples, it is clear a second reaction stage after 25 minutes of reaction in which the reaction rate decreases. This fact might be attributed to the control of the reaction by the internal diffusion of reactants and products within the mesoscopic channels. Anyway the effect of deactivation of the acid sites by adsorption of organic compounds should not be discarded to explain the decrease of activity obtained in this second stage. Nevertheless, the high absolute epoxide conversion (ca. 60 %) attained for Al-MCM-41 (2) after 25 minutes of reaction might also explain the marked decrease of the activity for this catalyst as a consequence of the substrate disappearance.

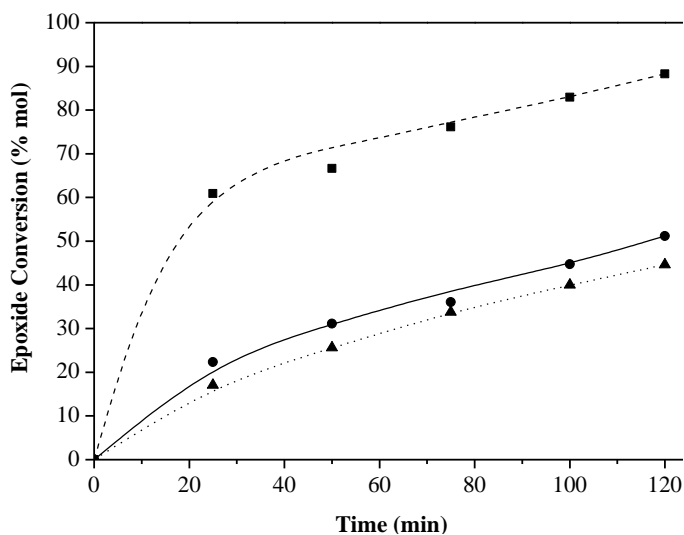


Figure 5. Epoxide conversion vs. reaction time in the isophorone oxide rearrangement over different Al-MCM-41 at 80 °C. (●) Al-MCM-41 (1), (■) Al-MCM-41 (2), (▲) Al-MCM-41 (3).

Figure 6 shows the molar product distribution obtained in isophorone epoxide rearrangement over Al-MCM-41 catalysts with different aluminium content. It is remarkable

that, regardless the catalysts used, the main reaction product was 2-formyl-2,4,4-trimethylcyclopentanone (3) with selectivities around 80-90%, whereas 3,5,5-trimethyl-1,2-cyclohexanedione (2) selectivities ranged from 10 to 20%. Consequently, these results indicate that the presence of an additional substituent in the β -position of cyclic α,β -epoxy ketones, such as isophorone oxide, when mesoporous acid materials are used as catalysts, favours the acyl migration resulting in ring contraction and therefore in the formation of the aldehyde over hydrogen migration leading to the α -diketone. Besides, Al-MCM-41 materials hinder the deformylation of 2-formyl-2,4,4-trimethylcyclopentanone (3), since 2,4,4-trimethylcyclopentanone (4) selectivities are almost negligible.

Although conversion was found to be dependent on the Si/Al ratio of Al-MCM-41 materials, reaction products selectivities hardly vary with the aluminium content of the catalysts or with the reaction time. As it can be seen in Figure 6, the selectivities towards the three reaction products detected were similar over the three Al-MCM-41 catalysts tested and varied slightly with the course of the reaction. In this way, selectivities towards 3,5,5-trimethyl-1,2-cyclohexanedione (2), 2-formyl-2,4,4-trimethylcyclopentanone (3) and 2,4,4-trimethylcyclopentanone (4) were set around 16%, 80% and 4%, respectively.

In conclusion, liquid phase isophorone oxide rearrangement over Al-MCM-41 type mesostructured materials leads to high yields (up to 80%) towards keto aldehyde (3) after 2 h of reaction, together with a low formation of the α -diketone (2) and negligible selectivities towards the decarbonylation product (4). Considering epoxide conversion, the best catalytic performance is obtained over Al-MCM-41 material with a molar Si/Al ratio of ca. 40. This catalyst combines appropriate pore size and amount of acid sites yielding a 90% epoxide conversion and aldehyde selectivity of ca. 80% after 2 h of reaction.

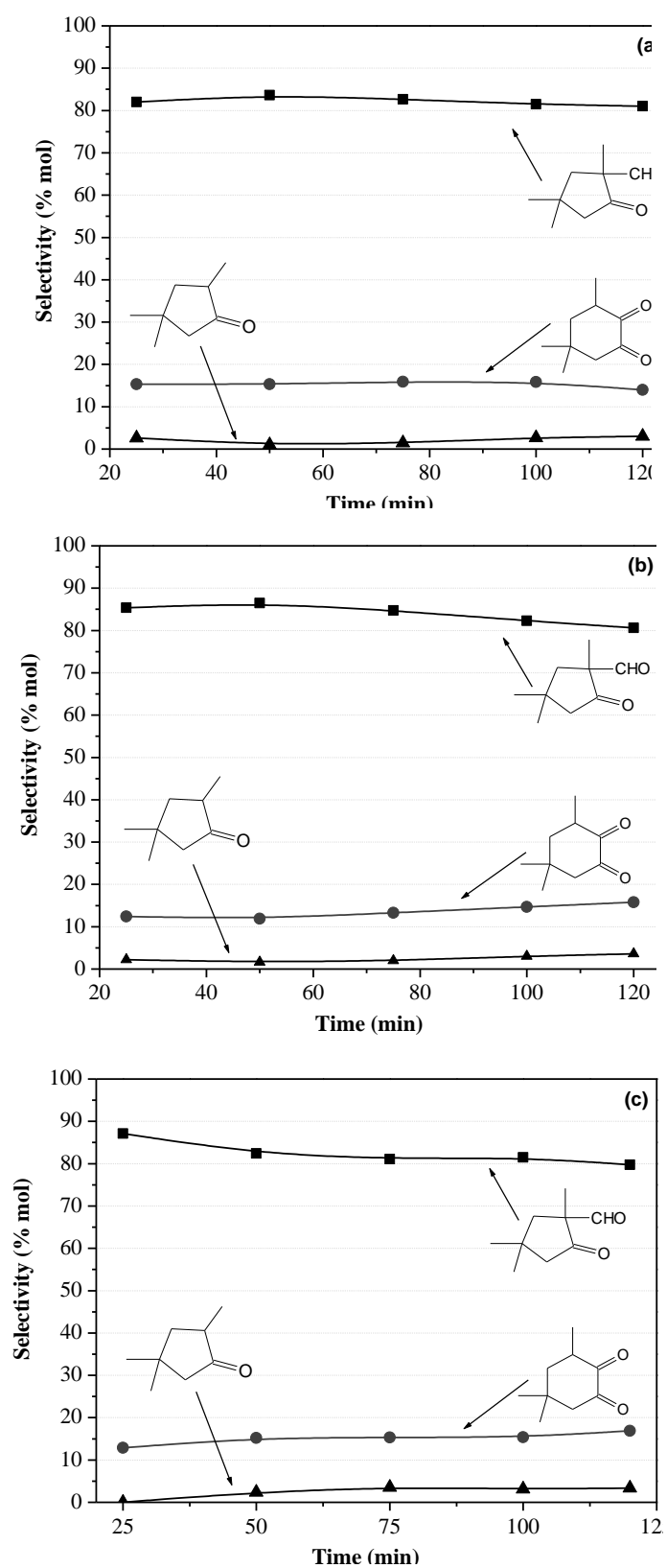
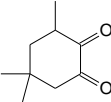
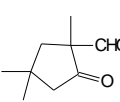
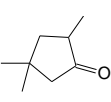


Figure 6. Molar product distribution obtained in isophorone epoxide rearrangement over Al-MCM-41 type mesostructured materials at 80 °C: (a) Al-MCM-41 (1), (b) Al-MCM-41 (2), (c) Al-MCM-41 (3).

In order to study the influence of temperature over the extent of the reaction, isophorone oxide rearrangement was studied over the Al-MCM-41 (2) catalyst at 60, 80 and 100°C (Table 2). The reaction time was 25 min with the purpose of obtaining comparative epoxide conversions. The main product was 2-formyl-2,4,4-trimethylcyclopentanone (3) with selectivities around 80% regardless of temperature, although the results in Table 2 show that the deformylation process seems to be slightly favoured with the temperature increase. As expected, the conversion is enhanced with the increase of the temperature. It is remarkable that isophorone epoxide conversion at 100°C over Al-MCM-41 materials reaches values close to 100% for a reaction time of just 25 min with high aldehyde selectivity.

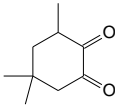
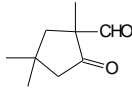
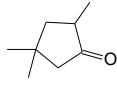
Table 2. Effect of reaction temperature on isophorone epoxide rearrangement over Al-MCM-41 (2).

Temperature (°C)	Conversion ^a (%)	Selectivity (%) ^a		
		 (2)	 (3)	 (4)
60	29.6	18.9	79.1	2.0
80	60.9	12.4	85.4	2.2
100	87.9	14.1	77.5	8.4

^a Reaction time = 25 min.

Finally, the results obtained in the present work have been compared with those published by Hoelderich et al. [26] in the liquid phase isophorone oxide rearrangement over zeolitic materials (see Table 3). Most of zeolites tested yielded complete conversion at 110 °C, although with long reaction times (6 h). The activity of ZSM-5 and Ferrierite is probably related to the acid sites located in the outer surface of the zeolite crystals. Indeed, the external acid sites may probably influence the activity showed by all the zeolites tested.

Table 3. Liquid phase rearrangement of isophorone oxide over zeolites (data adapted from reference [26])^a.

Catalyst	Conversion (%)	Selectivity (%)		
		 (2)	 (3)	 (4)
ZSM-5 (28)	88	14	68	1
ZSM-5 (60)	95	15	68	0
Al-BEA (25)	100	13	68	14
USY (70)	96	12	73	0
USY (96)	100	11	74	1
Ferrierite (18)	100	12	81	0

^a Reaction conditions: t = 6 h; T = 110°C; solvent: toluene; loading: 10 g isophorone oxide/g catalyst; the numbers in parentheses correspond to the SiO₂/Al₂O₃ ratios.

Although, the previous results show that zeolites catalyse efficiently the rearrangement of isophorone oxide to 2-formyl-2,4,4-trimethylcyclopentanone, it is worthy to compare them with the catalytic results obtained in this work using Al-MCM-41 materials as catalysts. Molar product distribution obtained over Al-MCM-41 (2) catalyst at different temperatures (see Table 2) show that Al-containing mesostructured materials yield high selectivities to the valuable product keto aldehyde (3), with values even higher to those obtained over ferrierite and USY zeolites. Moreover, Al-MCM-41 materials present much higher activities since they yield isophorone epoxide conversion close to 100% under reaction conditions similar to those used with zeolites (100°C; solvent: toluene; 12.5 g isophorone oxide/g catalyst), but with very short reaction times (25 minutes). These results can be assigned to the larger pores of mesostructured materials that avoid the diffusional problems present in zeolitic catalysts.

Conclusions

Al-MCM-41 materials effectively catalyze isomerization of isophorone oxide towards 2-formyl-2,4,4-trimethylcyclopentanone which is an useful compound for the synthesis of perfumes and synthetic flavours. The epoxide conversion is directly related with the pore size and amount of acid sites of Al-MCM-41 catalysts. A Si/Al molar ratio of ca. 40 is an optimal value, which combines an appropriate number of acid sites and pore diameter. For all the catalysts, selectivity towards the aldehyde decreases slightly with the reaction time, with values of ca. 80 % being obtained after 2 hours of reaction. The temperature affects the epoxide conversion but it does not modify significantly the product distribution. The aluminium-containing mesostructured catalysts display a high activity and selectivities toward the aldehyde isomer as compared with zeolitic materials.

References

1. J. Marc, *Advanced Organic Chemistry*, John Wiley & Sons, New York, 1985.
2. K. Arata, K. Tanabe, *Bull. Chem. Soc. Jpn.* 53 (3) (1980) 299.
3. J. G. Buchanan and H. Z. Sable, *Selective Organic Transformations*, John Wiley & Sons, New York, 1972.
4. W.F. Hölderich, H. van Bekkum, *Stud. Surf. Sci. Catal.*, 137 (2001) 821.
5. W.F. Hölderich in: R. A. Sheldon, H. van Bekkum (Eds.), *Fine Chemicals through Heterogeneous Catalysis*, Wiley/VCH, Weinheim, 2001, p. 217.
6. T-L Ho, S-H Liu, *Synth. Commun.* 13 (1983) 685.
7. M. Asaoka, S. Hayashibe, S. Sonoda, H. Takei, *Tetrahedron* 47 (1991) 6967.
8. H. O. House, *J. Am. Chem. Soc.* 76 (1954) 1235; H. O. House, R. L. Wasson, *J. Am. Chem. Soc.* 78 (1956) 4394; H. O. House, R. L. Wasson, *J. Am. Chem. Soc.* 79 (1957) 1488; H. O. House, G. D. Ryerson, *J. Am. Chem. Soc.* 83 (1961) 979.
9. H. O. House, D. J. Reif, R. L. Wasson, *J. Am. Chem. Soc.* 79 (1957) 2940.
10. R. D. Bach, M. W. Tubergen, R. C. Klix, *Tetrahedron Lett.* 27 (1986) 3565.
11. T. B. Rao, J. M. Rao, *Synth. Commun.* 23 (1993) 1527.
12. C. Meyer, W. Laufer, W. F. Hölderich, *Catal. Lett.* 53 (1998) 131.
13. J. A. Elings, H. E. B. Lempers, R. A. Sheldon, *Stud. Surf. Sci. Catal.* 105 (1997) 1165; J. A. Elings, H. E. B. Lempers, R. A. Sheldon, *Eur. J. Org. Chem.* (2000) 1905.
14. C. T. Kresge, M. E. Leonowicz, W. J. Roth, J. C. Vartuli and J.S. Beck, *Nature* 359 (1992) 710.
15. A. Corma, A. Martínez, V. Martínez-Soria, J. B. Montón, *J. Catal.* 153 (1995) 25.
16. D. P. Serrano, J. Aguado, J. L. Sotelo, R. van Grieken, J. M. Escola, and J. M. Menéndez, *Stud. Surf. Sci. Catal.* 117 (1998) 437.
17. C. Ngamcharussrivichai, P. Wu, T. Tatsumi, *J. Catal.* 227 (2004) 448.

18. L. Forni, C. Tosi, G. Fornasari, F. Trifirò, A. Vaccari, J. B. Nagy, *J. Mol. Catal. A: Chem.* 221 (2004) 97.
19. N. T. Mathew, S. Khaire, S. Mayadevi, R. Jha, S. Sivasanker, *J. Catal.* 229 (2005) 105.
20. D. B. Ravindra, Y. T. Nie, S. Jaenicke, G. K. Chuah, *Catal. Today* 96 (2004) 147.
21. D. P. Serrano, R. van Grieken, J. A. Melero, A. García, *Appl. Catal. A: General* 269 (2004) 137.
22. R. van Grieken, D. P. Serrano, J. A. Melero, A. García, *J. Mol. Catal. A: Chem.* 222 (2004) 167.
23. J. Aguado, D. P. Serrano, J. M. Escola, *Microporous Mesoporous Mater.* 34(2000) 43.
24. D. P. Serrano, J. Aguado, J. M. Escola, E. Garagorri, *Chem. Commun.* (2000) 2041.
25. R. D. Bach, R.C. Klix, *Tetrahedron Letters* 26 (1985) 985.
26. C. Meyer, W. Laufer, W. Hölderich, *Catal. Lett.* 53 (1998) 131.